

Z.Y. Yan  
B.T. Yang  
Z.C. Wang  
J.F. Xian  
M. Li

# Primary Chordoma in the Nasal Cavity and Nasopharynx: CT and MR Imaging Findings

**BACKGROUND AND PURPOSE:** Primary chordoma in the nasal cavity and nasopharynx is an extremely rare tumor in the extraosseous axial skeleton. Unlike intracranial chordomas, lesions in these sites primarily present as a soft tissue mass without involvement of the skull base bone (clivus), so the preoperative diagnosis of the tumor is possibly difficult. Here, we reviewed the imaging features of 5 cases of chordomas in the nasal cavity and nasopharynx that resulted in successful diagnosis and differential diagnosis of this rare tumor.

**MATERIALS AND METHODS:** We retrospectively studied 5 patients with histologically proven chordomas in the nasal cavity and nasopharynx. The lesion features of CT and MR imaging were reviewed, with emphasis on the size, shape, location, margin, calcification, CT attenuation characteristics, signal intensity, and degree of MR imaging enhancement.

**RESULTS:** Expansile and lobular soft tissue masses were mainly present, with irregular intratumor calcification in all 5 cases on CT examination. MR imaging revealed a well-defined tumor with heterogeneous signal intensity in 4 patients, whereas homogeneous signal intensity in 1 patient was present on all pulse sequences. Four cases of nasopharyngeal mass showed mild to moderate heterogeneous enhancement. Intratumor septa could be seen in 2 cases.

**CONCLUSIONS:** Although no imaging features are pathognomonic, primary chordomas without skull base (clivus) bony changes in the nasal cavity and nasopharynx have some CT and MR imaging findings that are suggestive of diagnosis. The differential diagnosis of the soft tissue mass should be limited to these sites.

**ABBREVIATIONS:** CE = contrast enhancement; heter = heterogeneous; homo = homogeneous; hyper = hyperintense; hypo = hypointense; Iso = isointense; SI = signal intensity; T1WI = T1-weighted image; T2WI = T2-weighted image

Chordomas are rare malignant tumors of notochordal origin and may occur at any site along the course of the embryonic notochord. These tumors typically occur in the axial skeleton and have a proclivity for the sphenoccipital region of the skull base and sacral regions with bony changes. Imaging features of chordomas elsewhere in the body have been reported in previously published literature.<sup>1-3</sup> The clinical findings of chordomas in the nasopharyngeal region only have been mentioned as an extension from an intracranial tumor in some studies.<sup>4-6</sup> The literature on CT and MR imaging of primary chordomas in the nasal cavity and nasopharynx is rather sparse.<sup>7-10</sup> The tumor usually presents in this region as a soft tissue mass with no change in the skull base bone (clivus) and is misdiagnosed as another tumor type. This study reviews CT and MR findings of 5 cases of chordomas with no clivus destruction in the nasal cavity or nasopharynx seen from 2004 to 2008 in our hospital, in an effort to improve the value of the differential imaging features of these unusual lesions.

## Materials and Methods

### Patients and Clinics

During the last 5 years (2004–2008), the cases of 5 patients with histologically proven chordomas were reviewed on the basis of electronic

data in our hospital, after approval from the Institutional Review Board. The data revealed 6 patients (0.67%) with chordomas in approximately 890 cases of a primary mass in the nasal cavity and nasopharynx. During the same period, 5 of these 6 patients had both CT and MR imaging findings. There were 1 female and 4 male patients, ranging in age from 6 to 66 years. The main symptoms and signs were nasal obstruction and congestion, headache, and soft tissue mass. Two patients experienced hearing loss.

CT examination was performed on a single-row detector CT scanner (Somatom Plus 4; Siemens, Malvern, Pennsylvania) in 5 patients. The scanner parameters were as follows: 120 kV and 200 mAs; table speed, 7.5 mm/s; and matrix, 256 × 256. Axial and coronal images were obtained with bone and soft tissue algorithm reconstruction. Section thickness and intersection gap were 2 and 5 mm, respectively.

MR imaging with an 8-channel head coil was performed on a 1.5T Signa Twinspeed scanner (GE Healthcare, Milwaukee, Wisconsin) in our hospital. MR imaging of 1 patient (case 1) was completed in another hospital; therefore, the type of scanner equipment (field strength) is unclear. Routine spin-echo T1-weighted images (TR, 450 ms; TE, 12 ms; NEX, 2; matrix, 288 × 224 pixels; section thickness, 4 mm; intersection gap, 0.4 mm; and FOV, 180 × 180 mm) and fast spin-echo T2-weighted images (TR, 4000 ms; TE, 110 ms; NEX, 3; matrix, 288 × 224 pixels; section thickness, 4 mm; intersection gap, 0.4 mm; and FOV, 180 × 180 mm) were acquired in the axial and coronal planes. T1-weighted sequence after gadolinium contrast administration was acquired in 4 patients (cases 2–5). Gadolinium-diethylene-triamine pentaacetic acid (0.2 mL/kg) was administered at a rate of 2.0 mL/s through a 22-gauge intravenous line with a power injector. After injection, axial, sagittal, and coronal T1-weighted

Received April 20, 2009; accepted after revision July 1.

From the Departments of Radiology (Z.Y.Y., B.T.Y., Z.C.W., J.F.X.) and Pathology (M.L.), Capital Medical University, Beijing Tongren Hospital, Beijing, China.

Please address correspondence to Zhenchang Wang, MD, Department of Radiology, Capital Medical University, Beijing Tongren Hospital, Beijing, China; e-mail: zhongyu\_yan@163.com

DOI 10.3174/ajnr.A1802

**Clinical presentation: CT and MR imaging findings of 5 patients with nasal and nasopharyngeal chordomas**

Age/ Sex	Location	Morphology	Extension Margin	CT Findings			MR Findings			Clinical
				Bone Involvement	Calcification	Density	T1WI SI	T2WI SI	Degree of CE	
M/6	Left nasal cavity	Expansible mass	Left ethmoid sinus; well- defined	Minimal	Linear	Iso; homo	Iso; homo	Hyper; heter	Not performed	Nasal obstruction from birth
M/38	Nasopharynx	Lobular mass	Bilateral posterior nasal choanal; well-defined	No	Irregular	Iso; heter	Iso; homo	Hyper; heter	Mild	Nasal obstruction for 2 years
M/13	Nasopharynx	Lobular mass	Left para- nasopharyngeal space; well- defined	No	Irregular	Iso; heter	Hypo; heter	Hyper; heter	Moderate	Headache, bilateral hearing loss for 5 years
F/66	Nasopharynx	Lobular mass	Left para- nasopharyngeal space; well- defined	No	Nodular	Iso; heter	Hypo; homo	Hyper; heter	Moderate	Headache for 1 year
M/31	Nasopharynx	Expansible mass	Nasopharynx; well-defined	No	Irregular	Iso; heter	Hypo; homo	Hyper; homo	Mild	Nasal obstruction for 2 years

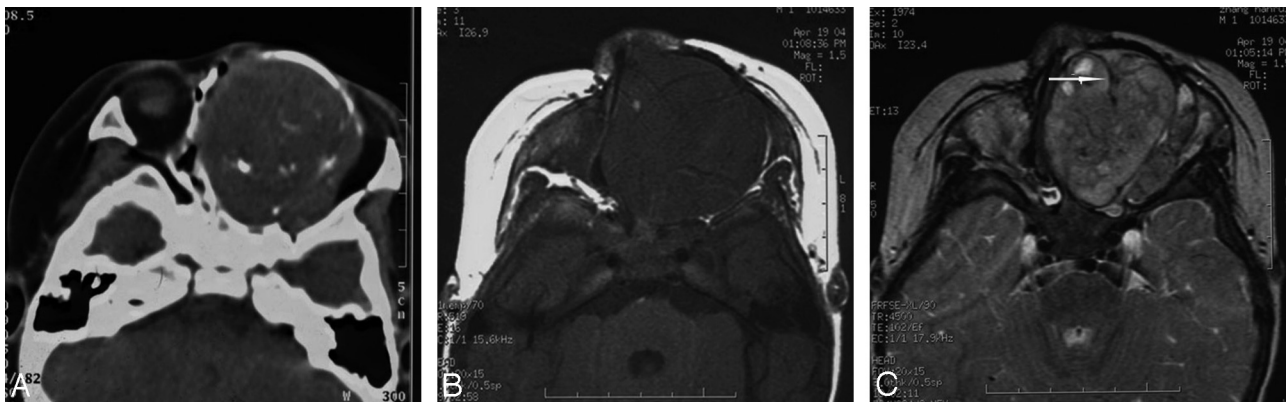


**Fig 1.** Case 1. Chordoma in the left nasal cavity in a 6-year-old boy. The tumor is an expansible and well-defined soft tissue mass with linear calcification in the left cavity on CT images (A). Compared with adjacent muscles, the tumor demonstrates hypointensity on spin-echo T1-weighted images (B), hyperintensity on T2-weighted images (C) with clear margins. Hypointense septa (arrow) can be seen on T2-weighted images.

images with fat saturation were acquired with the same parameters as the nonenhanced T1-weighted images.

Compared with adjacent muscles, the attenuation of CT and the signal intensity of MR imaging were evaluated. Other imaging findings are also described in the accompanying Table, including the location, morphology, extension and margin of the lesion, as well as bony involvement and the presence of intratumor calcification. After contrast administration, the enhancement was graded as mild, moderate, or marked degrees. The presence of hypointense septa was evaluated on T2-weighted images and contrast-enhanced T1-weighted images.

CT and MR images were reviewed by 2 experienced radiologists (Z. Y.Y. and B.T.Y.) by consensus concerning imaging features.

**Results**

Clinical histories of the 5 cases are summarized in the Table. The 5 patients had undergone complete excision and have remained well for 3, 1, 2, 5, and 2 years, respectively, after diagnosis. All 5 patients were treated with combined surgery and endoscopic surgery, without any postoperative radiation therapy administered. Tumors recurred in 4 cases at the time

of 1-year follow-up after surgery; 1 patient had no recurrence with improvement of nasal obstruction.

The CT and MR imaging features of the patients with chordomas are summarized in the Table. The tumors were primarily located in the left nasal cavity in 1 case and in the nasopharyngeal region in 4 cases. The maximal diameter ranged from 4.6 to 8.2 cm (mean, 6.4 cm), and the minimal diameter ranged from 2.5 to 6.0 cm (mean, 4.0 cm). All cases showed a soft tissue component with no obvious bone involvement in the clivus. Expansible and irregular masses with well-defined margin and focal calcification are the suggestive features.

With respect to adjacent muscles, the masses showed attenuation of muscles with low attenuation on CT imaging in 5 cases. MR imaging of the tumors revealed heterogeneous signal intensity in 4 cases and homogeneous signal intensity in 1 case. On T1-weighted images, the signal intensity of the tumors were isointense in 2 cases and hypointense in 3 cases, whereas on T2-weighted images, the lesions exhibited mixed hyperintensity in 4 cases and homogeneous hyperintensity in 1 case (Figs 1 and 2). Low-intensity strands on T2-weighted images corresponding to fibrous septa could be seen in 2 cases

HEAD & NECK ORIGINAL RESEARCH

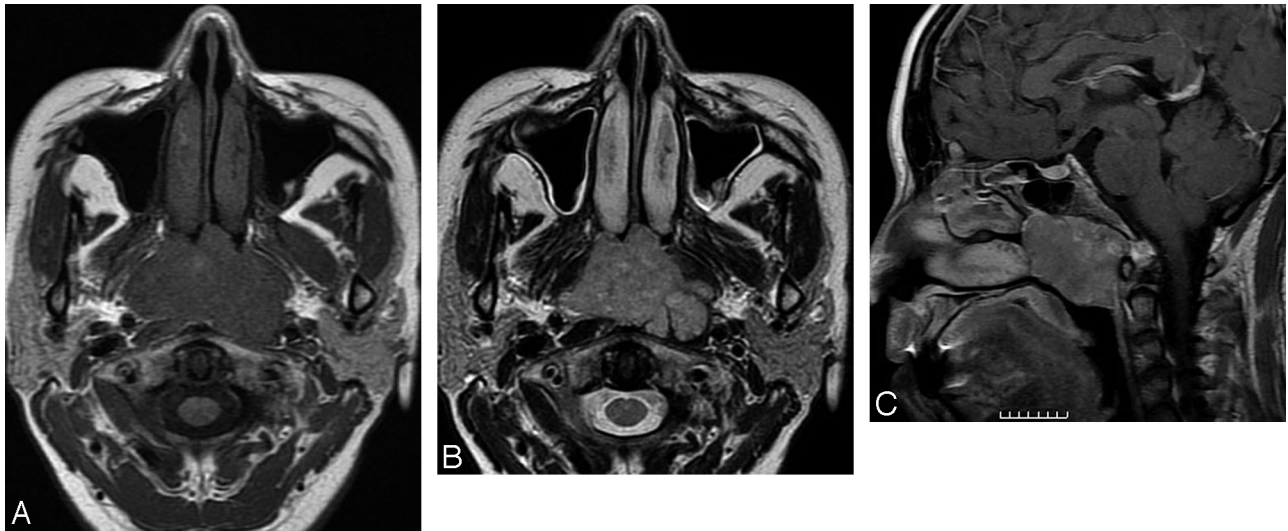


**Fig 2.** Case 2. Chordoma in the nasopharyngeal region in a 38-year-old man. Compared with adjacent muscles, the tumor shows isointensity on T1-weighted images (A), homogeneous hyperintensity on T2-weighted images (B), and mild heterogeneous enhancement on postcontrast T1-weighted images (C), with clear margins with adjacent structures. The clivus is uninvolved and has a normal appearance.

(Fig 1C). Except for 1 case, in which an enhancing examination was not performed for reasons unknown, the other 4 cases showed heterogeneous enhancement to a mild to moderate degree after gadolinium injection.

### Discussion

Intracranial chordomas most often originate from the sphenoid-occipital synchondrosis of the clivus<sup>11</sup> and primarily present as a soft tissue mass with bone destruction in the skull base. Rarely, chordomas may arise from the nasopharynx,<sup>2</sup> maxilla,<sup>12</sup> and paranasal sinuses. When this happens, it is difficult to differentiate a chordoma from other tumors in the nasal cavity and nasopharynx. In the view of imaging features, tumors arising from the clivus, with extension into the nasopharynx and nasal cavity, are not included in the list of primary chordomas.

Chordomas may occur at any age but are usually seen in adults, with peak prevalence in the fourth decade of life. Intracranial chordomas have a 2:1 male predilection.<sup>13,14</sup> Our group consisted of 4 males and 1 woman (age range, 6–66 years). It is usually difficult to make a diagnosis of primary chordomas in the nasal cavity and nasopharynx through endoscopic examination and on clinical findings. In our group (except for 1 case), the tumors originated in the left nasal cavity; 4 tumors appeared as nasopharyngeal soft tissue masses and bulged into the posterior nasal choanal region; and, in 2 cases, there was fluid in the mastoid air cells secondary to obstruction of the ostium of the eustachian tube. Also, the tumors recurred in 4 cases. Weber et al<sup>15</sup> reported distant metastases of intracranial chordomas to the lung, liver, bone, or lymph nodes with a proportion of 7% to 14%, whereas no metastases were observed in our study.

All lesions in our group formed a predominantly lobular soft tissue mass delineated by a fibrous pseudocapsule, which, because of adjacent tissue compression, accounted for the imaging appearance of being crisply marginated. Fluid and a gelatinous mucoid substance, associated with recent and old hemorrhages, and necrotic areas were found within the tu-

mor. The variety of these components may explain the signal intensity heterogeneity observed on MR imaging.<sup>16</sup> On microscopic examination, the notochord tissue is somewhat similar to immature cartilage and is composed of oval cells with central nuclei and a vacuolated cytoplasm embedded in an eosinophilic myxomatous stroma. The characteristic physaliphorous cells form the hallmark of chordomas.<sup>17</sup>

The 5 cases in our group revealed no bony involvement into the clivus, with only a large soft tissue mass in the nasal cavity and nasopharyngeal region. These localizations are best explained by the occurrence of extraosseous notochordal rests.<sup>18</sup> Remnants of these notochordal branches that have penetrated these sites presumably provide the seed from which subsequent ectopic chordomas may grow.<sup>19,20</sup>

The appearance of chordoma on CT images was that of a well-circumscribed, expansible soft tissue mass that arises from the nasal cavity, with linear calcification in 1 patient. In 4 patients, the lesions showed predominantly lobular morphologic features in the nasopharyngeal area with irregular focal calcification. Among them, 1 case showed minimal sequestra suggesting bony destruction. However, intratumoral high intensity could be seen in 4 cases. The high attenuation of the tumor showed an irregular appearance (Fig 3). We postulate that the attenuation most probably represents intratumoral calcification rather than bone sequestra because there were no bony structures in the sites; this needs to be confirmed by immunohistologic studies. Solitary or multiple low-attenuation areas are sometimes seen within the soft tissue mass and probably represent the myxoid and gelatinous material seen on gross examination.<sup>21,22</sup>

MR imaging provides excellent tissue contrast and exquisite anatomic details for radiologic evaluation of the nasal cavity and nasopharyngeal tumors. Compared with adjacent muscles, 5 cases revealed hypointensity or isointensity on T1-weighted images, and 4 lesions were heterogeneous. On T2-weighted images, 5 cases exhibited high heterogeneous signal intensity, a finding that likely reflects the high fluid content of vacuolated cellular components, as reported in the litera-

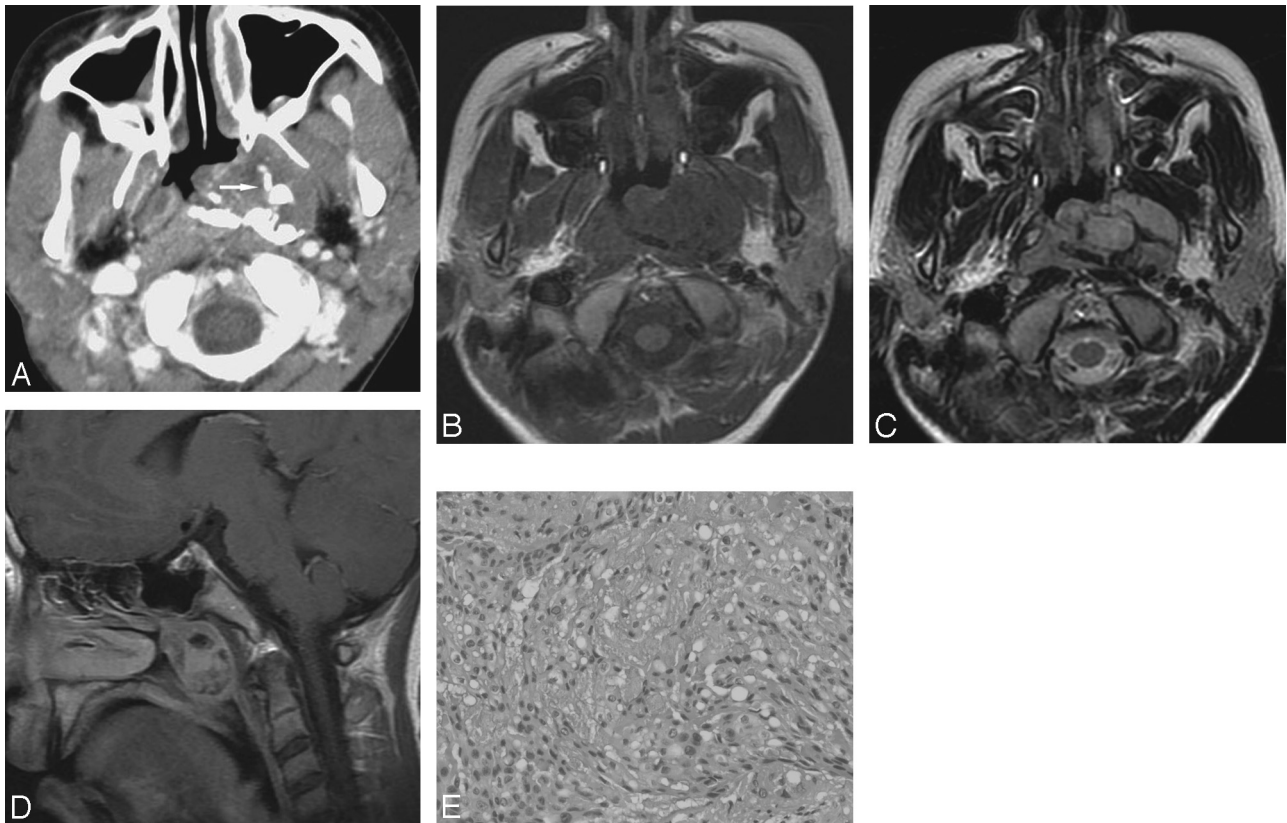


**Fig 3.** Case 3. Chordoma in the nasopharynx in a 13-year-old boy misdiagnosed with nasopharyngeal angiofibroma by nasal endoscopy. In the nasopharynx and left paranasopharyngeal space, the lobulated tumor exhibits irregular calcification (*arrow*) on CT images (A), isointensity on T1-weighted images (B), heterogeneous hyperintensity on T2-weighted images (C), and mild heterogeneous enhancement on postcontrast T1-weighted images (D), with clear margins with adjacent structures. The clivus has a normal signal intensity and appearance. The characteristic physaliphorous cells with large, sharply delimited, clear vacuoles imparting a bubbly appearance form the hallmark of chordoma (hematoxylin-eosin, original magnification  $\times 400$ ; E).

ture.<sup>23</sup> Intratumoral areas of calcification, hemorrhage, and a highly proteinaceous mucous pool usually demonstrate heterogeneous hypointensity on T2-weighted images (Fig 3). The fibrous septa that divide the gelatinous components of the tumor were clearly seen on the T2-weighted images as areas of low signal intensity. These septa have been reported in 70% of chordomas and are characteristic features of chordomas.<sup>24</sup> However, we only found these in 2 of 5 patients. Four cases of chordoma demonstrated mild to moderate enhancement after contrast material injection. The enhancement pattern of the tumor sometimes has a “honeycomb” appearance created by intratumoral areas of low signal intensity.<sup>25</sup> This pattern of contrast enhancement can reflect the pathologic features of such tumors, which are organized in lobules with mucinous and gelatinous contents.

However, MR imaging is deficient in the evaluation of calcification and cortical bone. Use of contrast-enhanced imaging can demonstrate osseous destruction if the tissue on the opposite side of the bone shows abnormal enhancement, which confirms bone involvement though the cortex is not actually visualized. Fat suppression may be useful for differentiation of enhanced tumor margins from adjacent fatty bone marrow. Combined CT and MR imaging is the desirable technique for the diagnosis and pretreatment evaluation.

Because of the definite location of the nasal cavity and nasopharynx, the differential diagnosis of chordoma should be made from other nasopharyngeal and nasal soft tissue

masses. In the nasopharynx, 2 cases in the group were preoperatively misdiagnosed as nasopharyngeal carcinoma and juvenile nasopharyngeal angiofibroma. Usually, peak ages for the incidence of juvenile nasopharyngeal angiofibroma are within the second decade of life; these angiofibromas primarily arise from the region of the sphenopalatine foramen. Void of flow and considerable enhancement after injection of contrast material on MR imaging may support the diagnosis of the juvenile nasopharyngeal angiofibromas. A short history, predilection among the Asian population, bony destruction, and a soft tissue mass with limited calcification are the characteristics of nasopharyngeal carcinoma, and the nasopharyngeal mucosa is usually involved, as shown on postcontrast MR imaging. In the nasal cavity, the differential diagnosis between chordomas and chondrosarcoma is surely difficult on imaging and clinical examination. Some imaging features may be suggestive of chordoma including no destruction of the clivus, an expansible and lobular soft tissue mass with well-defined margins, and intratumor calcification.

### Conclusions

Primary chordoma in the nasal cavity and nasopharynx is a rare tumor and is usually misdiagnosed. Although CT and MR imaging features are nonspecific, they may be suggestive of chordoma, including a well-defined expansible or lobular soft tissue mass, focal amorphous calcification, intratumor septa, no destruction of the clivus, heterogeneous hyperintensity on

T2-weighted imaging, and mild to moderate enhancement. Although we have results in only a small group of patients, some CT and MR imaging features may reduce the number of the differential diagnoses for chordoma in the nasal cavity and nasopharynx.

## References

- Rosenthal D, Scott JA, Mankin HJ, et al. **Sacroccygeal chordomas: magnetic resonance imaging and computed tomography.** *AJR Am J Roentgenol* 1985;145:143–47
- Sung MS, Lee GK, Kang HS, et al. **Sacroccygeal chordomas: MR imaging in 30 patients.** *Skeletal Radiol* 2005;34:87–94
- Wippold FJ 2nd, Koeller KK, Smirniotopoulos JG. **Clinical and imaging features of cervical chordomas.** *AJR Am J Roentgenol* 1999;172:1423–26
- Firooznia H, Pinto R, Lin J, et al. **Chordomas: radiologic evaluation of 20 cases.** *AJR Am J Roentgenol* 1976;127:797–805
- Omerod R. **A case of chordomas presenting in the nasopharynx.** *J Laryngol Otol* 1960;74:245–54
- Eisemann ML. **Sphenooccipital chordomas presenting as a nasopharyngeal mass. A case report.** *Ann Otol Rhinol Laryngol* 1980;89:271–75
- Scartozzi R, Couch M, Sciubba J. **Chondroid chordomas of the nasal septum.** *Arch Otolaryngol Head Neck Surg* 2003;129:244–46
- Singh N, Soo M, De Cruz M, et al. **Cervical chordomas presenting as retropharyngeal mass and dysphonia: case report and literature review.** *Australas Radiol* 2007;51 Suppl:B183–88
- Porret C, Mom T, Llompant X, et al. **[Cervical and para-pharyngeal bone tumors: two cases report.]** *Ann Otolaryngol Chir Cervicofac* 2005;122:295–302
- Gormley WB, Beckman ME, Ho KL, et al. **Primary craniofacial chordomas: case report.** *Neurosurgery* 1995;36:1196–99
- Mirra J, Nelson S, Della Rocca C, et al. **Chordomas.** In: Fletcher CD, Unni K, Mertens F, eds. *Pathology and Genetics of Tumors of Soft Tissue and Bone.* Lyon, France: IARC Press; 2002:316–17
- Shugar JM, Som PM, Krespi YP, et al. **Primary chordomas of the maxillary sinus.** *Laryngoscope* 1980;90:1825–30
- Mizerny BR, Kost KM. **Chordomas of the cranial base: the McGill experience.** *J Otolaryngol* 1995;24:14–19
- Dorfman HD, Czerniak B. **Bone cancers.** *Cancer* 1995;75(1 Suppl):203–10
- Weber AL, Brown EW, Hug EB, et al. **Cartilaginous tumors and chordomas of the cranial base.** *Otolaryngol Clin North Am* 1995;28:453–71
- De Beuckeleer LH, De Schepper AM, Ramon F, et al. **Magnetic resonance imaging of cartilaginous tumors: a retrospective study of 79 patients.** *Eur J Radiol* 1995;21:34–40
- Inci S, Palaoglu S, Onol B, et al. **Low cervical chordomas: a case report.** *Spinal Cord* 1996;34:358–60
- D'Haen B, De Jaegere T, Goffin J, et al. **Chordomas of the lower cervical spine.** *Clin Neurol Neurosurg* 1995;97:245–48
- Yoneoka Y, Tsumanuma I, Fukuda M, et al. **Cranial base chordomas—long term outcome and review of the literature.** *Acta Neurochir (Wien).* 2008;150:773–78
- Lipper MH, Cail WS. **Chordomas of the petrous bone.** *South Med J* 1991;84:629–31
- Meyer JE, Oot RF, Lindfors KK. **CT appearance of clival chordomas.** *J Comput Assist Tomogr* 1986;10:34–38
- Whelan MA, Reede DL, Meisler W, et al. **CT of the base of the skull.** *Radiol Clin North Am* 1984;22:177–217
- Erdem E, Angtuaco EC, Van Hemert R, et al. **Comprehensive review of intracranial chordomas.** *Radiographics* 2003;23:995–1009
- Murphy JM, Wallis F, Toland J, et al. **CT and MRI appearances of a thoracic chordoma.** *Eur Radiol* 1998;8:1677–79
- Doucet V, Peretti-Viton P, Fiquella-Branger D, et al. **MRI of intracranial chordomas: extent of tumor and contrast enhancement—criteria for differential diagnosis.** *Neuroradiology* 1997;39:571–76